DOI: 10.1002/ejic.200900511

# $Tm^{3+}$-Doped $Y_2O_3$ Nanocrystals: Rapid Hydrothermal Synthesis and Luminescence

**Murukanahally Kempaiah Devaraju,*[a] Shu Yin,[a] and Tsugio Sato[a]**

**Keywords:** Hydrothermal synthesis / Nanostructures / Luminescence / Lanthanides / Thulium / Yttrium

$Tm^{3+}$-doped $Y_2O_3$ nanocrystals were prepared via hydrothermal conditions at high autogenous pressure (ca. 40 MPa) using batch reactors at 220 and 250 °C for very short periods of reaction time (10 min). The as-prepared materials were identified as $Y(OH)_3$ nanoparticles. The precursor materials with two types of morphologies, such as sphere and rod-shaped particles were prepared at 220 and 250 °C within 10 min. The sizes of the as-prepared sphere particles are 10–15 nm in diameter, whereas the rod-shaped particles show 15–20 nm in diameter and 0.1–0.2 μm in lengths. The precursor materials were calcined at 500 and 800 °C for 5 h in air to obtain (3 mol-%) $Tm^{3+}$-doped $Y_2O_3$ nanocrystals. For the characterization, XRD, FESEM, EDS and TG-DTA were employed. The photoluminescence spectra of sphere and rod-shaped particles show higher blue emission at 450 nm than the reference sample.


## Introduction

Rare earth phosphors are extensively applied in luminescence and display, such as fluorescent lamps, projection television tubes, field emission display (FED), and plasma display panels (PDP).[1,2] $Tm^{3+}$-doped crystals are especially interesting since they can be excited by ultra-stable laser diodes and can be used as eye-safe and diode-pumped solid-state lasers. Particularly, $Tm^{3+}$-doped phosphors have potential applications in high definition television (HDTV) and plasma display panels.[3] Nowadays, nanocrystalline rare earth phosphor materials are receiving extensive attention due to their unusual properties and potential applications. Especially, control over both nanocrystalline morphologies and the crystal sizes is a new challenge to synthetic chemists and materials scientists.[4] During the last decade, morphology control of various kinds of materials in nanoscale or microscale was widely investigated because of their special applications in optoelectric and other fields.[5–9]

Recently our group has reported on the morphology-controlled synthesis of europium-activated $Y_2O_3$ nanoparticles under supercritical conditions.[10] Over the last decade, many methods for the synthesis of rare earth oxide doped $Y_2O_3$ phosphors have been reported, including solution combustion method,[11] sol-gel method,[12] spray pyrolysis method,[13] hydrothermal synthesis[14] precipitation method[15] and solvothermal refluxing method.[16,17] Among the many different methods listed above, hydrothermal synthesis meets the increasing demand for the direct preparation of crystalline ceramic powders and offers a low temperature alternative to conventional powder synthesis technique in the production of anhydrous oxide powders. This technique can produce fine, high purity, stoichiometric particles of single and multicomponent metal oxides.[18] Although, many reports are available on $Eu^{3+}$-doped $Y_2O_3$ nanomaterials but the limited work has been reported on controlled morphology synthesis of blue-emitting $Tm^{3+}$-activated phosphors.[16,19,20] In this paper, we describe the synthesis of $Tm^{3+}$-doped $Y_2O_3$ nanomaterials and the room temperature photoluminescence of structurally different $Tm^{3+}$-doped $Y_2O_3$ nanomaterials. So far, rare earth phosphors prepared via conventional hydrothermal method required more than 1 hour to form precursor materials for the preparation of phosphors. The present hydrothermal method using batch reactors at high autogenous pressure (ca. 40 MPa) offers a facile and fast route for the synthesis of inorganic nanoparticles.

The morphology-controlled synthesis of $Tm^{3+}$-doped $Y_2O_3$ materials via hydrothermal method has not yet been reported. In this article a hydrothermal method for the preparation of sphere- and rod-shaped nanoparticles in very short reaction time is described. The product morphology can be controlled by tuning the reaction temperature. The effect of reaction time and effect of the dopant were investigated. The room temperature photoluminescence property of $Tm^{3+}$-doped $Y_2O_3$ nanomaterials were compared with the reference sample prepared via conventional co-precipitation method.

[a] Institute of Multidisciplinary Research for Advanced Materials, Tohoku University,
2-1-1, Katahira, Aoba-ku, Sendai 980-8577, Japan
Fax: +81-22-217-5597
E-mail: devaraju@mail.tagen.tohoku.ac.jp
devarajumk@rediffmail.com

  

## Results and Discussion

### Phase Formation

Figure 1 (see parts a and b) shows the XRD pattern of as-prepared samples at 220 and 250 °C under hydrothermal conditions at 220 and 250 °C and at autogenous pressure (ca. 40 MPa) for 10 min. The sample exhibited strong diffraction and all the reflections can be readily indexed with a pure hexagonal phase [$P6_{3/m}$] of $Y(OH)_3$ with lattice constants $a$ = 0.6248, and $c$ = 0.3524, which is well agreed with the literature values of $a$ = 0.6268, $c$ = 0.3547 (JCPDS 24-1422). According to X-ray diffraction data, there are no differences in the peak positions observed between the two samples. The as-prepared samples at 220 and 250 °C were calcined above at 800 °C to obtain a pure cubic phase [$Ia_3$] of $Y_2O_3$, confirmed by the XRD pattern as shown in Figure 1 (c, d). The XRD pattern indicates that pure $Y(OH)_3$ can be obtained under hydrothermal conditions and followed by calcinations to obtain $Y_2O_3$ nanospheres and nanorods.

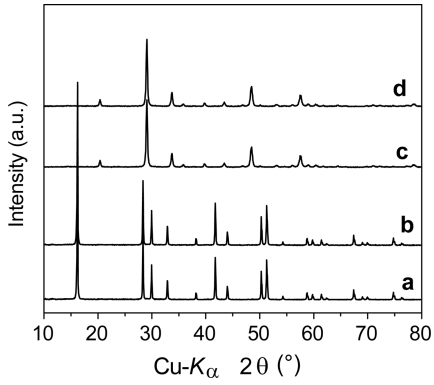


Figure 1. XRD patterns of as-prepared $Y(OH)_3$ particles (a and b), and $Tm^{3+}$:$Y_2O_3$ particles after calcination at 800 °C for 5 h in air (c and d).

### Thermal Stability

Parts a and b of Figure 2 show the TG-DTA profile of as-prepared samples at 220 and 250 °C, respectively. The samples showed 2 steps weight loss about 20% was observed and indicating that $Y_2O_3$ was produced by two-step dehydration of $(YOH)_3$ during the calcinations process. The weight loss is associated with two endothermic peaks between 280–450 °C as shown in Figure 2 (a, b).

### Samples Morphology

The morphology and sizes of as-prepared and calcined samples were investigated by FESEM. The FESEM images of as-prepared and calcined samples are shown in Figure 3 (a–f). The as-prepared sample at 220 °C for 10 min consists of monodispersed sphere particles with 10–15 nm diameter (Figure 3, a). The calcined samples at 500 °C and 800 °C show well-dispersed sphere morphology with increasing in

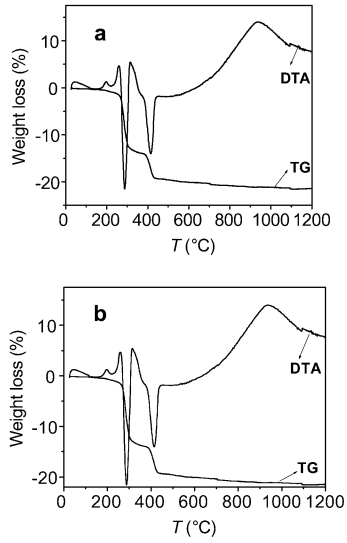


Figure 2. TG-DTA curves of as-prepared sphere particles (a) at 220 °C, and rod-like particles (b) at 250 °C, for 10 min, respectively.

particles sizes, i.e., 20–30 and 50–60 nm for the samples calcined at 500 and 800 °C for 5 h in air, respectively (Figure 3, b and c). The as-prepared sample at 250 °C shows rod-shaped particles with 15–20 nm in diameter size and lengths of 0.1 to 0.2 μm as shown in Figure 3 (d). The diameter and lengths of the rod-shaped particles increases after calcinations at 500 and 800 °C. The sample calcined at 500 °C is 20–30 nm in diameter and 0.3 μm long as depicted in Figure 3 (e). The samples calcined at 800 °C is 40–70 nm in diameter and have lengths up to 0.5 μm as shown in Figure 3 (f).

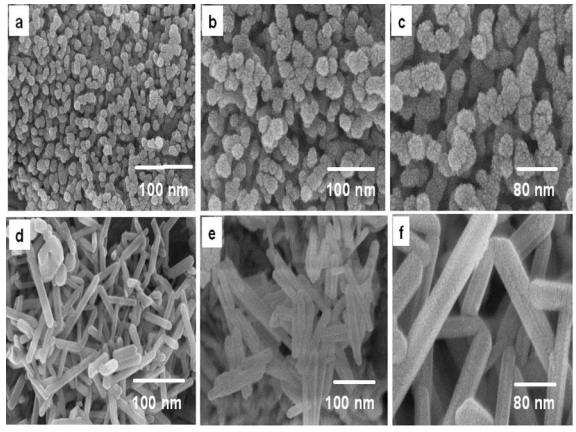


Figure 3. FESEM images of as-prepared sphere and rod-like particles (a and d) and then calcined at 500 °C (b and e), and 800 °C (c and f) for 5 h in air, respectively.

Further, the influence of the reaction time on the morphology of as-prepared sphere and rod-shaped samples was investigated. Figure 4 (a–c) shows the samples prepared at different reaction times (5, 15, and 20 min). The 5-min-sample consists of fine and hard agglomerated particles (see Figure 4, a). When the reaction time was increased to 15 min, sphere particles were obtained with 10 nm in diameter size and particles are partly agglomerated as shown

  

in Figure 3 (b). Further increase of reaction temperature to 20 min leads to the formation of hard agglomerated particles as shown in Figure 4 (c). The effect of reaction time on rod-shaped particle was also investigated. When the reaction time is 5 min, very fine agglomerated particles are observed as shown in Figure 4 (d). The mixture of sphere and rods were obtained after 15 min of reaction time as shown in Figure 4 (e). Further, increase of the reaction time to 20 min leads to the formation of elongated rods (see Figure 4, f). The optimum reaction time to form monodispersed sphere particles and rod-shaped particles is 10 min. The hydrothermal synthesis carried out using a morrey-type autoclave at the desired temperature and at atmospheric pressure (1 atm) required more than 5 h of reaction time to form crystalline materials,[21,22] but in the present hydrothermal synthesis, we have synthesized the precursor materials within a very short period of reaction time by using batch reactors that can withstand high autogenous pressure (ca. 40 MPa).

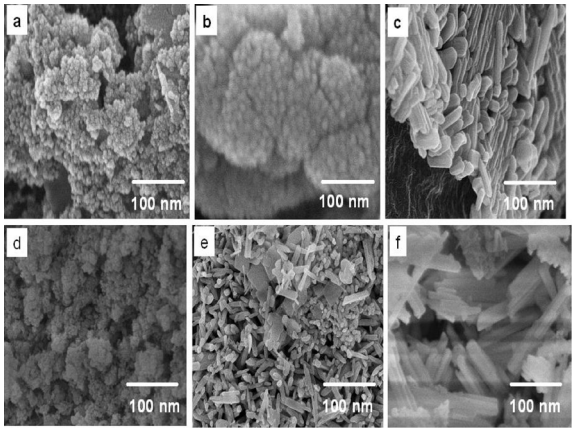


Figure 4. FESEM images of as-prepared samples at 220 °C (a–c) and 250 °C (d–f), for 5 min (a and d), 15 min (b and e) and 20 min (c and f), respectively.

The formation of sphere and rod-shaped particles occurs through the nucleation of $Tm^{3+}$:$Y(OH)_3$ nanoparticles under hydrothermal condition at high autogenous pressure (40 MPa). The sphere particles are formed due to the slow growth rate. When the growth rate is fast, the nanoparticles continue to grow upon increase of reaction temperature under high autogenous pressure to form rod-shaped particles with a hexagonal cross section due to its anisotropic hexagonal structure, similar to that of ZnO.[23]

The presence of elements, such as Tm, Y and O were confirmed in as-prepared and calcined sample at 500 °C by EDS analysis. Figure 5 (a) shows the EDS spectra of as-prepared $Tm^{3+}$-doped $Y(OH)_3$ nanospheres, and Figure 5 (b) shows the EDS spectra of $Tm^{3+}$-doped $Y_2O_3$ after calcinations at 800 °C for 5 h in air.

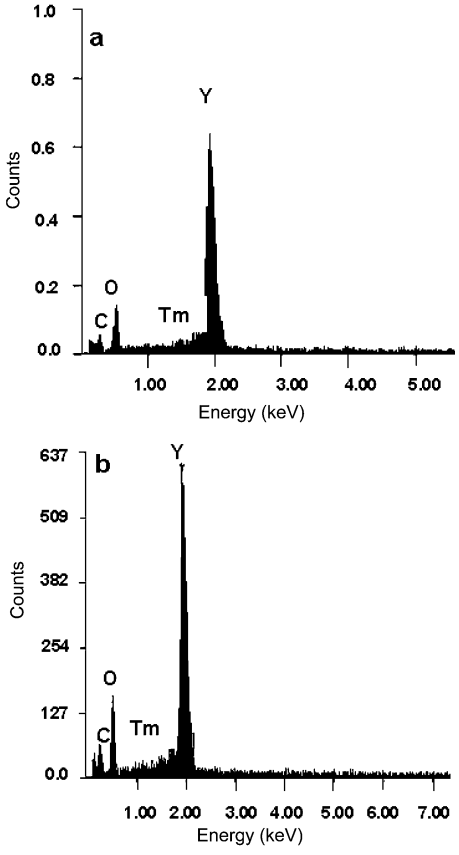


Figure 5. EDS spectra of as-prepared $Tm^{3+}$:$Y(OH)_3$ at 220 °C (a), and calcined $Tm^{3+}$:$Y_2O_3$ (b).

## Photoluminescence of $Tm^{3+}$:$Y_2O_3$ Nanospheres and Nanorods

The photoluminescence emission spectra of 3 mol-% $Tm^{3+}$-doped $Y_2O_3$ nanospheres and nanorods are shown Figure 6 (a and b). The emission intensity exhibited by nanospheres after calcination at 500 and 800 °C for 5 h is more than that of nanorods. The emission intensities of rod-shaped particles and sphere-shaped particles after calcination at 500 °C is lower than that of the samples calcined at 800 °C and this increased emission intensity might be due to the increased crystallinity of rod-shaped particles and sphere-shaped particles after calcination at 800 °C for 5 h in air. The samples exhibited blue emission around 450 nm under the excitation wavelength of 360 nm. The blue emission from the $Tm^{3+}$-doped $Y_2O_3$ nanospheres and nanorods are corresponds to $^1D_2 \rightarrow {}^3F_4$ electron transition.[16,24] The highest emission intensity exhibited by $Tm^{3+}$-doped $Y_2O_3$ nanospheres after calcinations at 800 °C for 5 h in air, which is probably due to the increase of crystal size, and well occupied $Tm^{3+}$ ions in the $Y_2O_3$ host lattice. Usually, sphere particles exhibits strong photoluminescence intensity due to spherical morphology, narrow size distribution and nonagglomeration. The emission intensity of both samples is more than that of the reference sample prepared by the co-precipitation calcination method. The reference sample was calcined at 800 °C for 5 h in air. The emission intensity of 3 mol-% $Tm^{3+}$-doped $Y_2O_3$ nanospheres and nanorods are increased with rising the calcination temperature for nanospheres and nanorods, respectively.

  

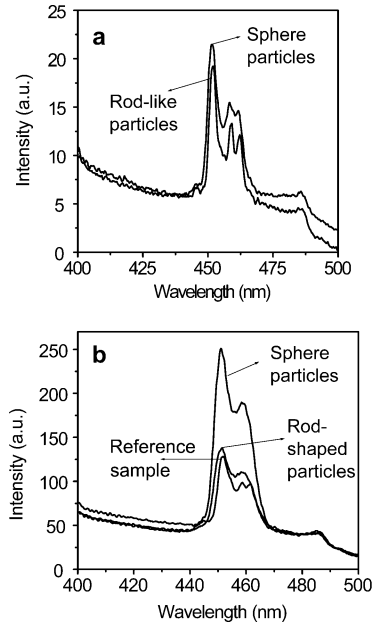


Figure 6. PL spectra of (3 mol-%) $Tm^{3+}$:$Y_2O_3$ and reference sample after calcinations at 500 °C (a), and 800 °C (b), for 5 h in air, respectively.

Furthermore, the effect of the $Tm^{3+}$ content in $Y_2O_3$ samples was investigated. Figure 7 shows the PL spectra of 0.5, 1, 1.5, 2.5 and 3.5 mol-% of $Tm^{3+}$-doped $Y_2O_3$ samples calcined at 800 °C for 5 h in air. The emission intensity for both nanospheres and nanorods increased up to 3 mol-% as shown in Figure 7. The quenching effect was observed for 3.5 mol-% doped samples. The quenching effect might due to cross-relaxation and resonance between the activators ions ($Tm^{3+}$) and also due to paired activator ions ($Tm^{3+}$).

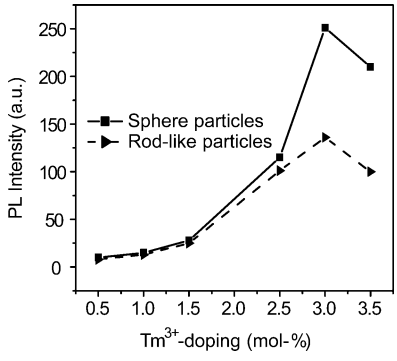


Figure 7. Effect of $Tm^{3+}$-doping on PL intensity.

## Conclusions

In summary, $Tm^{3+}$-doped $Y_2O_3$ nanomaterials were prepared with two kinds of morphologies: sphere and rod morphology via hydrothermal route and a postcalcining process. The morphology, crystal structure, thermal stability, elemental analysis, and photoluminescence property were characterized by XRD, FESEM, TG-DTA, EDS, and PL. The effect of reaction time on morphology was investigated. The as-prepared materials were identified as $Y(OH)_3$ nanoparticles by powder X-ray diffraction. The sizes of the sphere particles are 10–20 and 20–60 nm in diameter before and after calcinations. The rod-shaped particles show 20–30 nm in diameter and less than 0.3 μm in lengths for precursor materials, 30–70 nm in diameter and 0.3–0.5 μm in lengths for calcined samples, respectively. The pressure, reaction temperature and reaction time are the key factors in preparing sphere and rod-shaped nanoparticles. The strong blue emission at 450 nm (excitation wavelength 360 nm) were observed for sphere particles after calcinations at 800 °C, which is highest when compared to rod-shaped particles and the reference sample. The investigation of effect of doping of $Tm^{3+}$ ion into $Y_2O_3$ host showed 3 mol-% is the optimum percentage, as quenching effect was observed around 3.5 mol-% $Tm^{3+}$ ions.

## Experimental Section

**General:** The phase composition of samples was determined by X-ray diffraction analysis (XRD, Shimadzu XD-D1) using graphite-monochromatized Cu-$K_\alpha$ radiation. The calcination temperature of the sample was determined by thermogravimetry-differential thermal analysis (TG-DTA, Rigaku TAS-200). The morphology and size of the samples were determined by FESEM analysis (Hitachi S4800). EDS spectra were obtained on Hitachi S4800. The photoluminescence spectra and intensity were measured by a spectrofluorophotometer (Shimadzu RF-5300P) at room temperature.

**Synthesis of $Y_2O_3$:$Tm^{3+}$ (3 mol-%) Nanospheres and Nanorods:** $Y_2O_3$:$Tm^{3+}$ (3 mol-%) nanoparticles with sphere- and rod-shaped morphologies were prepared under hydrothermal conditions at 220 and 250 °C and at autogenous pressure (ca. 40 MPa) for 10 min. In a typical synthesis, 30 mL of 0.05 M $YCl_3$ aqueous solution and 0.015 mmol $TmCl_3$, corresponding to 3 mol-% $Tm^{3+}$-doping were put in a beaker and stirred for about 15 min. Then, 10 mL of an aqueous solution of 2 M KOH was added and the mixed solution was stirred for few min to form a white colloidal solution. After that, 10 mL of the colloidal solution was transferred to a batch reactor with 20 mL of internal volume, and the reactors were heated with reciprocally shaking at a rate of 50 revolutions/min at 220–260 °C for about 10 min, and then the reactors were submerged in cold water, cooled to room temperature. The resulting product was collected, washed with water, and vacuum dried at 60 °C. $Tm^{3+}$-doped $Y_2O_3$ nanoparticles were prepared by calcination of the as-prepared product at above 500 °C for 5 h in air.

The reference sample was prepared using 0.05 M $YCl_3$ aqueous solution and 0.015 mmol $TmCl_3$, and then dilute ammonia solution was added to get the precipitate. The resulted white precipitate was separated by centrifugation and dried. The dried product was calcined at 800 °C for 5 h in air to obtain desire 3 mol-% $Tm^{3+}$-doped $Y_2O_3$ powder.

## Acknowledgments

This research was partially supported by the Ministry of Education, Culture, Sports, Science and Technology, Japan (Scientific Research of Priority Areas, "Panoscopic Assembling and High Ordered Functions for Rare Earth Materials", Special Education and Research Expenses on "Post-Silicon Materials and Devices

  

Research Alliance") and the Japan Society for the Promotion of Science (JSPS) Asian Core Program (Program: "Interdisciplinary Science of Nanomaterials").

[1] T. Hase, T. Kano, E. Nakazawa, H. Yamamoto, *Adv. Electron. Electron Phys.* **1990**, *79*, 271–373.
[2] G. Blasse, B. C. Grabmaier, *Luminescent Materials*, Springer, Berlin, **1994**.
[3] R. P. Rao, *J. Lumin.* **2005**, *113*, 271–278.
[4] G. Zhu, P. Liu, J. Zhou, X. Bian, X. Wang, J. Li, B. Chen, *Mater. Letters.* **2008**, *62*, 2335–2338.
[5] W. U. Huynh, J. J. Dittmer, A. P. Alivisatos, *Science* **2002**, *295*, 2425–2427.
[6] M. H. Huang, S. Mao, H. Feick, H. Q. Yan, *Science* **2001**, *292*, 1897–1899.
[7] F. Caruso, *Chem. Eur. J.* **2000**, *6*, 413–419.
[8] A. Vecht, C. Gibbons, D. Davies, *J. Vac. Sci. Technol. B* **1999**, *17*, 750–757.
[9] M. Law, H. Kind, B. Messer, F. Kim, P. Yang, *Angew. Chem.* **2002**, *114*, 2511–2514.
[10] M. K. Devaraju, S. Yin, T. Sato, *J. Cryst. Growth* **2009**, *311*, 580–584.
[11] W. W. Zhang, M. Xu, W. P. Zhang, M. Yin, Z. M. Qi, S. D. Xia, G. Claudine, *Chem. Phys. Lett.* **2003**, *376*, 318–323.
[12] M. K. Chong, K. Pita, C. H. Kam, *J. Phys. Chem. Solids* **2005**, *66*, 213–217.
[13] K. Y. Jung, K. H. Han, *Electrochem. Solid-State Lett.* **2005**, *8*, H17–20.
[14] P. K. Sharma, M. H. Jilavi, R. Nab, H. Schmidt, *J. Mater. Sci. Lett.* **1998**, *17*, 823–827.
[15] Y. He, Y. Tian, Y. F. Zhu, *Chem. Lett.* **2003**, *32*, 862–863.
[16] M. K. Devaraju, Shu Yin, Tsugio Sato, *IOP Conf. Series*: *Materials Science and Engineering 1*, **2009**, 012011, DOI:10.1088/1757-8981/1/1/012011.
[17] M. K. Devaraju, S. Yin, T. Sato, *Mater. Sci. Eng. C* **2009**, *29*, 1849–1854.
[18] D. S. Bae, K. S. Han, S. B. Cho, S. H. Choi, *J. Kor. Assoi. Cry. Grow.* **1997**, *7*, 167–170.
[19] K. J. B. M. Nieuwesteeg, C. A. H. A. Mutsaers, *Philips J. Res.* **1989**, *44*, 157–182.
[20] A. Daud, M. Kitagawa, H. Takeshima, H. Futaki, S. Tanaka, H. Kobayashi, *Jpn. J. Appl. Phys.* **1994**, *33*, L652–L655.
[21] Y. Mao, J. Y. Huang, R. Ostroumov, K. L. Wang, J. P. Chang, *J. Phys. Chem. C* **2008**, *112*, 2278–2285.
[22] J. Yang, Z. Quan, D. Kong, X. Liu, J. Lin, *Cryst. Growth Des.* **2007**, *7*, 730–735.
[23] Y. Xia, P. Yang, Y. Sun, Y. Wu, B. Mayers, B. Gates, Y. Yin, F. Kim, H. Yan, *Adv. Mater.* **2003**, *15*, 353–389.
[24] J. Hao, S. A. Studenikin, M. Cocivera, *J. Lumin.* **2001**, *93*, 313–319.

Received: June 9, 2009
Published Online: September 10, 2009

  